Effect of shape anisotropy on percolation of aligned and overlapping objects on lattices

Jasna C. K. [*] and V. Sasidevan [†]

Department of Physics, Cochin University of Science and Technology, Cochin 682022, India

We investigate the percolation transition of aligned, overlapping, anisotropic shapes on lattices. Using the recently proposed lattice version of excluded volume theory, we show that shape-anisotropy leads to some intriguing consequences regarding the percolation behavior of anisotropic shapes. We consider a prototypical anisotropic shape—rectangle—on a square lattice and show that, for rectangles of width unity (sticks), the percolation threshold is a monotonically decreasing function of the stick length, whereas, for rectangles of width greater than two, it is a monotonically increasing function. Interestingly, for rectangles of width two, the percolation threshold is independent of its length. We show that this independence of threshold on the length of a side holds for d-dimensional hypercubiods as well as for specific integer values for the lengths of the remaining sides. The limiting case of the length of the rectangles going to infinity shows that the limiting threshold value is finite and depends upon the width of the rectangle. This "continuum" limit with the lattice spacing tending to zero only along a subset of the possible directions in d dimensions results in a "semicontinuum" percolation system. We show that similar results hold for other anisotropic shapes and lattices in different dimensions. The critical properties of the aligned and overlapping rectangles are evaluated using Monte Carlo simulations. We find that the threshold values given by the lattice-excluded volume theory are in good agreement with the simulation results, especially for larger rectangles. We verify the isotropy of the percolation threshold and also compare our results with models where rectangles of mixed orientation are allowed. Our simulation results show that alignment increases the percolation threshold. The calculation of critical exponents places the model in the standard percolation universality class. Our results show that shape anisotropy of the aligned, overlapping percolating units has a marked influence on the percolation properties, especially when a subset of the dimensions of the percolation units is made to diverge.

I. INTRODUCTION

Percolation problems have commanded enduring interest in the realm of statistical physics, finding diverse applications in fields ranging from material science and polymer chemistry to epidemic spreading and financial markets [1–8]. The fundamental focus of percolation theory lies in investigating the connectivity properties of random and disordered media. In the simplest model of lattice site percolation, each site of a lattice is randomly occupied with a probability p. Clusters are formed by the nearest occupied sites, and as the occupation probability is gradually increased from zero, the system eventually reaches a point where the largest cluster spans the entire lattice, signaling the occurrence of percolation [9,10]. Percolation models can also be extended to continuum space, where geometric shapes or objects, which can partially or fully overlap, are randomly placed in the space with a specific number density. Some of the commonly considered shapes include disks, spheres, cubes, squares, and sticks [11–13]. Overlapping objects give rise to distinct clusters and, similar to lattice percolation, the system exhibits a phase transition, marked by the emergence of a spanning cluster at a critical

number density. Identifying the percolation threshold and characterizing the associated critical behavior constitute a major research theme in the study of various percolation systems [10]. The probability of forming a spanning cluster serves as one of the order parameters and the critical phenomenon is characterized by a power-law divergence of specific quantities close to the percolation threshold. Also, the universality of critical exponents is seen across many models of percolation [14].

Among the diverse variants of percolation on lattices, many recent studies have focused on the percolation of extended shapes that do not overlap [15–26]. Compared to this, there are only a few studies on extended shapes that overlap [27–30]. The models with overlapping shapes introduce multisite occupancy and/or multiple occupancy of a site, also serving as a natural bridge between various lattice and continuum models. For example, the percolation of overlapping squares and cubes on lattices was studied by Koza *et al.* [27], who focused on calculating the percolation thresholds of these models and their transition from discrete to continuum values. Percolation of discrete overlapping hyperspheres on hypercubic lattices was studied by Brzeski and Kondrat [29]. They studied the discrete-to-continuum transition of hyperspheres, which enabled the evaluation of the threshold for the three-dimensional (3D) and higher dimensional continuum problems with greater accuracy. Apart from these, recent

_____

[*]jasnack@cusat.ac.in

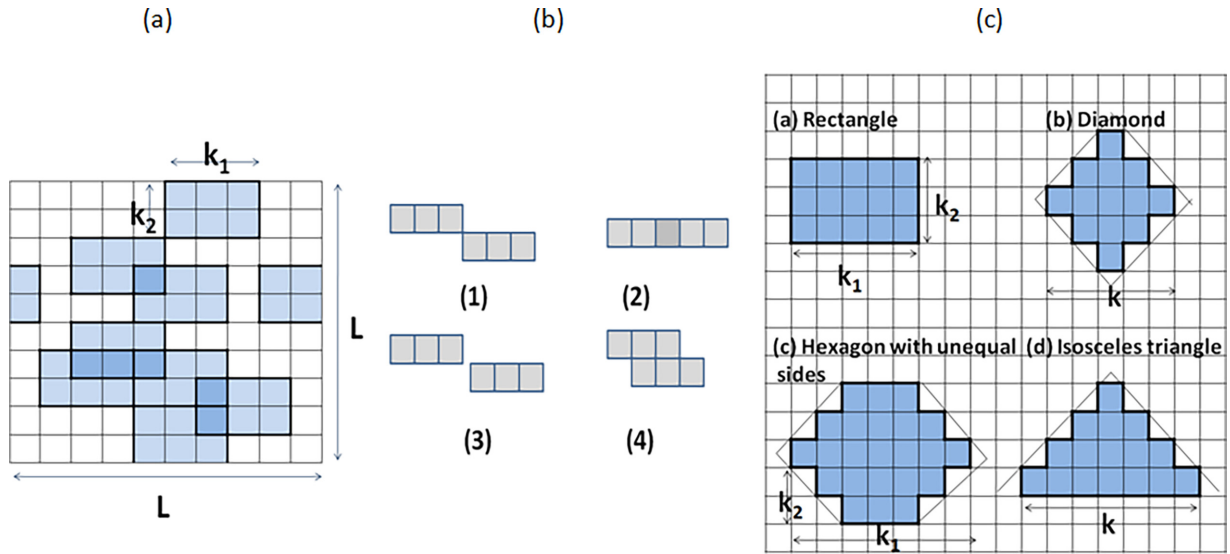[†]sasidevan@cusat.ac.in, sasidevan@gmail.com

FIG. 1. (a) Square lattice of size $L \times L$ with overlapping rectangles of length $k_1 = 3$ and width $k_2 = 2$ randomly distributed on it. Rectangles are aligned in the horizontal direction and can overlap. (b) Different possible arrangements of two rectangles with $k_1 = 3$ and $k_2 = 1$. (1) Two rectangles touching at corners are considered unconnected. (2) Two overlapping rectangles are considered connected. (3) Two nonoverlapping rectangles. (4) Two rectangles sharing edges are considered connected. (c) A few of the extended shapes possible on a square lattice are shown with their defining parameters marked. The name for a shape is given based on the shape of its outline.

studies focus on site percolation with extended neighborhoods, which can be mapped onto the problem of lattice percolation of extended and overlapping shapes like disks, squares, etc. [27,31,32].

Percolation models involving overlapping shapes, in addition to their theoretical significance, hold practical relevance in various applications. These models, applied to both lattice and continuum structures, serve as valuable tools for representing the structure of random and disordered media and investigating their diverse transport properties. The collective arrangement of overlapping shapes can represent either the material components or voids within a structure. For example, overlapping ellipses have been used for modeling composites of conductive nanoparticles dispersed in insulating matrices [33]. Similarly, electrical conductivity in nanocomposites has been studied using both soft-core (noninteracting) and hardcore (interacting) shapes [34]. Other examples include the study of nanocomposite materials consisting of conductive rodlike particles [35,36], systems consisting of conducting polymers [37,38], and composite fiber systems [39,40]. The latter gives a comparison between soft-core and hardcore models for fiber systems. Numerous real-world scenarios involve the flow of fluids or other conductive phenomena, such as electrical conductivity, in 2D structures [41–44]. In the past, studies have utilized 2D overlapping aligned rectangles, integrated with an underlying lattice structure, to analyze transport properties [45–49]. Apart from these examples, the fact that image analysis of a disordered material usually involves discretizing a continuous space makes the studies on lattices very much relevant in the context of random media [50]. Thus it is evident that the versatility and applicability of percolation models with overlapping shapes, both in 2D and 3D lattice structures, make them pertinent in understanding and characterizing various physical systems.

This paper delves into the percolation of overlapping and aligned anisotropic shapes on lattices. Specifically, as a prototypical example of such problems, we consider the percolation of aligned and overlapping "rectangles" on a two-dimensional square lattice in detail. In the particular case of either side of the rectangle being of unit length, we can call the shapes rods or sticks (see Fig. 1). Apart from their potential practical relevance, our main motivation behind considering this and other extended anisotropic shapes stems from the peculiar behavior of the percolation threshold of aligned and overlapping rectangles in the 2D continuum problem. In the latter, the percolation threshold remains independent of the rectangles' aspect ratio due to the affine symmetry of such systems [51]. In simple words, for such systems, scaling one or both directions will not change the connectivity properties of the system and, hence, will not change the percolation threshold. Similar invariance of percolation threshold under scaling also exists for disk percolation in continuum [52]. However, on lattices, such symmetry under scaling cannot be defined and we show that this leads to intriguing percolation behavior, which depends not just on the aspect ratio but on the specific values of the sidelengths of the aligned rectangles and other shapes.

Employing the excluded volume theory adapted to a lattice setting [27] and employing Monte Carlo simulations, we analyze the percolation of aligned and overlapping rectangles on the two-dimensional square lattice. We show that the lattice version of the excluded volume theory gives several intriguing predictions regarding the percolation threshold of such systems. For the specific case of aligned and overlapping rectangles, the value of the percolation threshold as we increase the length of the rectangles depends on its width. For width one rectangles, the threshold monotonically decreases with the length and, for width greater than two, it increases

monotonically. For width two, the threshold is independent of the length. This independence of threshold on the length of a side holds for d-dimensional hypercuboids also, for specific integer values for the lengths of the remaining sides. Moreover, we get a nonzero percolation threshold, even in the limiting case where one side of the rectangle extends to infinity while keeping the other side finite. We show that similar results hold for other shapes and dimensions as well and obtain predictions for both qualitative and quantitative behavior of the threshold for several such systems. The theory gives us good numerical estimates for the percolation thresholds for rectangles and other anisotropic shapes.

Our Monte Carlo simulation results confirm the theoretical predictions regarding the behavior of the percolation thresholds for aligned and overlapping rectangles. We verify that isotropy of the percolation threshold holds even with rectangles of large aspect ratios, just as in the continuum problem [51]. Additionally, critical exponents are obtained, demonstrating that the problem lies within the same universality class of lattice percolation. Furthermore, a comparison between results for aligned sticks and a mixture of sticks of varying orientations is presented, providing valuable insights into the impact of anisotropy on the percolation process.

The paper is organized as follows. In Sec. II, we precisely define the model of overlapping rectangles on a square lattice. In Sec. III, we use excluded volume theory adapted to a lattice setting to analyze the problem. We use the theory to draw conclusions about the percolation of extended shapes other than rectangles and also in other dimensions. We give the results of simulation studies. The percolation threshold is evaluated and results are compared. Isotropy of percolation threshold, critical exponents, and effect of mixed orientations are also given. We conclude in Sec. IV.

II. MODEL DEFINITION

In general, we look into the percolation problem of aligned, overlapping, anisotropic shapes in lattice systems. For concreteness, we consider the case in which each unit of percolating objects is a rectangle with sidelengths k_1 in the horizontal direction and k_2 in the vertical direction randomly positioned on a two-dimensional square lattice of size $L \times L$ (see Fig. 1). Without loss of generality, we will assume that $k_1 \geqslant k_2$ so that the rectangles are aligned in the horizontal direction.

The rectangles are allowed to overlap; hence a site can be occupied more than once—a feature known as multiple occupancy. However, the complete overlapping of two rectangles is avoided (note that the second rectangle does not contribute toward the total number of occupied sites). This will also retain the classical site percolation scenario when $k_1 = k_2 = 1$. Occupied neighboring sites are assumed to be connected, where the neighborhood is the von Neumann type. In other words, rectangles that share sites or are adjacent are considered connected entities and rectangles that touch only at corners are considered nonconnected [see Figs. 1(a) and 1(b)].

As the density of occupied sites, denoted by ϕ (the ratio of the total number of occupied sites and L^2), is progressively increased by adding more rectangles to the lattice, a critical point is reached where a spanning cluster emerges.

We define the spanning cluster as a connected path of rectangles in the vertical direction (perpendicular to the direction of alignment), signifying percolation in the system. Periodic boundary conditions are imposed in the horizontal direction. Snapshots of the typical configurations for different values of ϕ, with $k_1 = 3$ and $k_2 = 1$, are shown in Fig. 2.

The percolation threshold is the specific value of ϕ where the spanning cluster first arises, indicating the transition from a nonpercolating to a percolating state. ϕ_c may be considered the equivalent of the critical covered volume fraction (CCVF) in continuum percolation [11]. In continuum percolation theory, we have areal density η and covered area or volume fraction related to each other through $\phi = 1 - \exp(-\eta)$ [11]. Areal density is the net volume of all the objects per unit volume of the space and covered area fraction is the fraction of the total volume of space covered by the objects. The objects are randomly distributed in space; hence the probability that there are a certain number of objects in an area follows a Poisson distribution. Hence the probability that a point in space is not covered by any object is the same as the probability that there are no objects present within a volume equal to the volume of the object V (or average volume of objects if there is a size distribution for the objects) which is $\exp(-Vn)$, where n is the number density of objects. $\eta = Vn$ is the areal density. ϕ is then the probability that the point in space is covered by at least one object, which is $1 - \exp(-\eta)$. It is easily seen that the same arguments and relation hold for extended overlapping objects on lattices as well, with n now denoting the number density of objects on the lattice and V the "volume" of the object (the number of lattice sites occupied by one object). η is the equivalent of the area or volume density in continuum percolation. For convenience, we will use this terminology for the lattice percolation as well.

Note that when $k_1 = k_2 = k \to \infty$, the problem corresponds to the 2D continuum percolation problem of overlapping and aligned squares [27,28]. The problem may be defined with shapes other than rectangles and also for other types of lattices as well. For example, a few simple shapes that can be considered on the square lattice are shown in Fig. 1(c). We will discuss other extended shapes, lattices, and dimensions later in Sec. III A.

III. RESULTS AND DISCUSSION

A. Lattice version of excluded volume theory

A major quantity of interest in the problem is the percolation threshold, i.e., the value of ϕ at which the system percolates for given values of k_1 and k_2. A useful analytical approximation technique to obtain the percolation threshold of systems for which the shapes of the percolating units are similar is the excluded volume theory [53,54]. The excluded volume theory, initially proposed for continuum percolation systems, is based on the idea that the product of the number density of basic percolating units and the average excluded volume, which gives us the total excluded volume, is an invariant quantity for "similar systems" at the critical point. Similar systems here mean geometrically similar shapes that are distributed with a particular orientation [53]. For example, systems of squares and rectangles of a particular orientation.
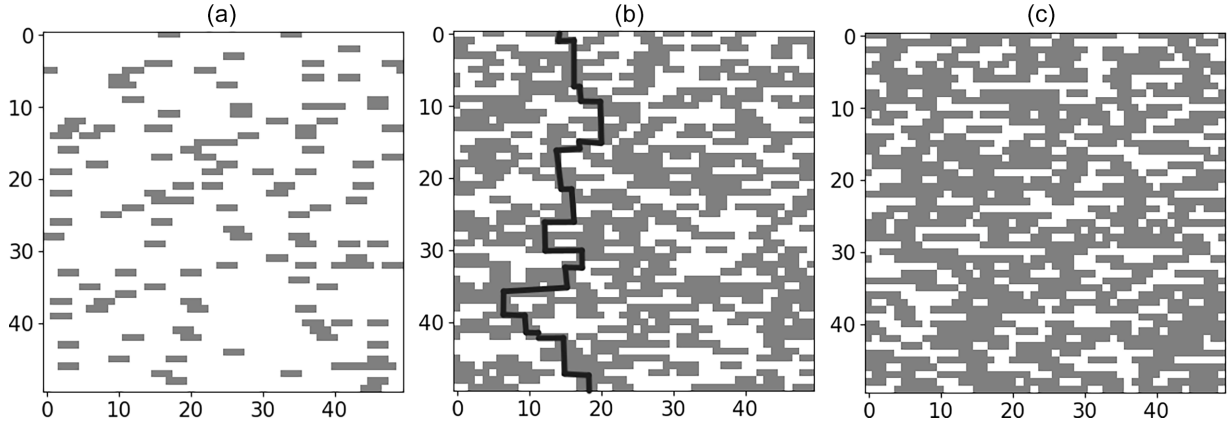
FIG. 2. Typical configurations obtained for rectangles of side lengths $k_1 = 3$, $k_2 = 1$ distributed randomly on an $L = 50 \times 50$ square lattice for different values of the density of occupied sites ϕ. The grid of the lattice is not shown for visual clarity. The gray color corresponds to the rectangles. The system is considered as percolating if there is connectivity from top to bottom via rectangles. (a) At $\phi = 0.14 < \phi_c$, the system is nonpercolating. (b) At $\phi = 0.56 \approx \phi_c$, the system is percolating with the first spanning cluster developed in the vertical direction. The percolating path connecting the top to the bottom is marked. (c) At $\phi = 0.64$, the system is well above the percolation threshold ϕ_c

In the continuum context, this means shapes that can be scaled to each other and have the same orientation. For shapes considered on a lattice, since there is no notion of scaling, we can say that two shapes are similar if their continuum limits can be scaled to each other and have the same orientation. Therefore, we expect the total excluded area to be the same for systems of oriented squares and oriented rectangles (see Ref. [55] for similar findings in a related context).

For continuum cases, the excluded volume is the volume around an object into which, if another object is placed, the two objects will overlap. Recently, the idea has been extended to lattice models as well, where the excluded volume is replaced by what is called the connectedness factor—the number of possible configurations of two basic percolating units such that they are connected—[27] (see Fig. 3). The connectedness factor will depend on the shape of the objects and also on their relative orientation. The lattice version of excluded volume theory thus says that the product of the number density of objects and the connectedness factor is a constant at criticality for similar systems where similarity refers to the shape and orientation of the basic percolating units. If n is the number density of objects (total number of objects divided by the total number of lattice points) and V_{ex} is the connectedness factor, then

$$n_c V_{ex} = B_c, \qquad (1)$$

where n_c is the number density at the critical point and B_c is the average number of connections an object has at criticality, which is approximately expected to take the same value for similar objects. Here, the number density $n = \eta/V$, where V is the volume (number of lattice sites occupied) of an object. Therefore, at criticality, we can write the CCVF,

$$\phi_c \approx 1 - \exp\left(-B_c \frac{V}{V_{ex}}\right). \qquad (2)$$

Now for rectangles of sides k_1 and k_2, V is simply $k_1 \times k_2$. We can find V_{ex} by enumerating the configuration of two rectangles such that they are connected. It is easily seen that $V_{ex} = (2k_1 + 1)(2k_2 + 1) - 5$ (see Fig. 3). Therefore, the

covered volume fraction at the critical point

$$\phi_c^{k1,k2} \approx 1 - \exp\left(-B_c \frac{k_1 k_2}{(2k_1 + 1)(2k_2 + 1) - 5}\right). \qquad (3)$$

So, unlike the continuum case, here the CCVF depends on the aspect ratio of the rectangles. We can recover the continuum case in the limit of both k_1 and k_2 much greater than unity for which the above expression becomes independent of k_1 and k_2:

$$\phi_c \approx 1 - \exp(-B_c/4). \qquad (4)$$

Several interesting inferences can be made from Eq. (3). Consider the case in which we take k_1 to be very large for a
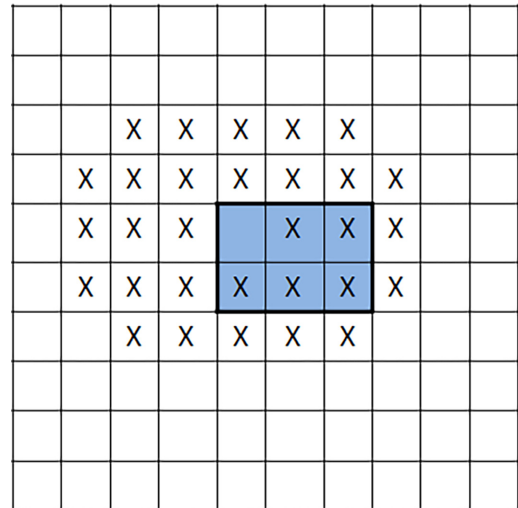

FIG. 3. If the top-left corner site of the rectangle is chosen as the index site (site with no cross mark), the cross-marked cells constitute the excluded area of the rectangle shown, which is of length $k_1 = 3$ and width $k_2 = 2$. That is, if the index site of another rectangle falls within this area, it will overlap with the rectangle shown in the figure. The excluded volume is $V_{ex} = (2k_1 + 1)(2k_2 + 1) - 5$. Note that exact overlapping of rectangles is not allowed.

fixed finite value of k_2. In the limit of $k_1 \to \infty$, the expression for CCVF becomes

$$\phi_c^{k_1 \to \infty, k_2} \approx 1 - \exp\left(-B_c \frac{k_2}{2(2k_2 + 1)}\right). \tag{5}$$

Equation (3) gives how the percolation threshold approaches the limiting value in Eq. (5) as we increase k_1. We can easily see that, for $k_2 = 1$, $\phi_c^{k_1, k_2}$ is a decreasing function of k_1, whereas, for $k_2 > 2$, $\phi_c^{k_1, k_2}$ is increasing in k_1. Now, for $k_2 = 2$, $\phi_c^{k_1, k_2}$ is independent of k_1, indicating that for overlapping and aligned rectangles of width two on a square lattice, the percolation threshold is independent of its length.

Equation (5) implies that, for rectangles with finite width and length tending to infinity, the percolation threshold is finite and depends on the width of the rectangles. Moreover, unlike squares whose infinite limit gives us the continuum percolation problem of squares, there seems to be no continuum problem corresponding to the case of rectangles with infinite length and finite width. This is true as long as we consider the case $k_1 \to \infty$ keeping k_2 a constant. We will discuss the transition to the continuum picture in more detail in Sec. III B 4.

It is interesting to note that, for the particular case of aligned overlapping sticks ($k_2 = 1$), the dependence of percolation threshold on stick length k_1 is given by $\phi_c \sim 1 - \exp(-B_c \frac{k_1}{3(2k_1+1)-5})$. We may compare and contrast this with the case of nonoverlapping stick percolation. The latter system is often predicted to have a power-law dependence of the percolation threshold on stick length $\phi_c \sim 1/k_1^\alpha$ [15,19] or an exponentially decreasing dependence [21].

We can easily see that similar results will hold for extended shapes in other types of lattices and dimensions. For example, consider the problem of overlapping and aligned cuboids on a cubic lattice. If the sidelengths of the cuboids are denoted by k_1, k_2, and k_3, then CCVF is given by

$$\phi_c^{k1, k2, k3} \approx 1 - \exp\left(-B_c \frac{k_1 k_2 k_3}{V_{ex}^{k_1, k_2, k_3}}\right), \tag{6}$$

where $V_{ex}^{k_1, k_2, k_3}$ is

$$V_{ex}^{k_1, k_2, k_3} = (2k_1 - 1)(2k_2 - 1)(2k_3 - 1)$$
$$+ 2[(2k_1 - 1)(2k_2 - 1) + (2k_1 - 1)(2k_3 - 1)$$
$$+ (2k_2 - 1)(2k_3 - 1)] - 1. \tag{7}$$

When all the sidelengths tend to infinity, we recover the continuum percolation threshold of aligned and overlapping cubes in 3D, given by

$$\phi_c = 1 - \exp\left(\frac{-B_c}{8}\right), \tag{8}$$

with appropriate values of B_c. From Eqs. (7) and (6), we can verify that, for $k_2 = 2$ and $k_3 = 4$ (or vice versa), the percolation threshold ϕ_c becomes independent of k_1. We can easily show that this set of values is unique. In Eq. (7), if we set $a_2 = (2k_2 - 1)$ and $a_3 = (2k_3 - 1)$; for ϕ_c to be independent of k_1, we require to have odd positive integer values of a_2 and a_3 greater than or equal to 3 that satisfy the relation $a_2 = \frac{2a_3+1}{a_3-2}$ (or $a_3 = \frac{2a_2+1}{a_2-2}$). Now if $a_3 = 3$, then $a_2 = 7$. For higher values of a_3, the ratio $\frac{2a_3+1}{a_3-2}$ is monotonically

decreasing and tends to 2 for large a_3. So for a higher value of a_3 to satisfy the above relation, the only remaining possibility is $a_2 = 5$. However, it is easy to verify that $a_2 = 5$ will not satisfy the relation for any integer value of a_3. This shows that the combinations $a_2 = 3$ and $a_3 = 7$ ($k_2 = 2$, $k_3 = 4$) or $a_2 = 7$ and $a_3 = 3$ ($k_2 = 4$, $k_3 = 2$) are the only possible set of integers which will make the threshold independent of k_1. We can generalize this to hypercuboids in d dimensions, where we expect ϕ_c to be independent of k_1 for a particular set of integer values of $k_2, k_3, \ldots, k_d$. For example, in four dimensions, $k_2 = 2$, $k_3 = 4$, and $k_4 = 22$ will make ϕ_c independent of k_1. Generalization of this result for d-dimensional hypercuboids and corresponding proof is given in Appendix A.

For the special case of thin sheets (say $k_2 \to \infty$ and $k_3 \to \infty$ with finite k_1), we get $\phi_c^{k_1} = 1 - \exp(-B_c \frac{k_1}{(8k_1+4)})$. For the special case of sticks in 3D (say $k_2 = k_3 = 1$ and finite k_1), we get $\phi_c^{k_1} = 1 - \exp(-B_c \frac{k_1}{5(2k_1-1)+1})$. Letting the length of the sticks go to infinity, i.e., considering $k_1 \to \infty$, we get the finite limiting value $\phi_c = 1 - \exp(-B_c/10)$. As in the case of rectangles on a 2D square lattice, where the limiting case of rectangles with finite width on the lattice does not give the continuum model of rectangles, the limiting case of anisotropic shapes in a 3D cubic lattice also does not give the corresponding continuum model. For example, for cubes and cuboids on a continuum, $\phi_c = 1 - \exp(-B_c/8)$, whereas the limiting value obtained for $k_1 \to \infty$ for sticks ($k_2 = k_3 = 1$) on a cubic lattice is $\phi_c = 1 - \exp(-B_c/10)$.

Considering the general case of overlapping and aligned sticks of length k_1 randomly placed on a hypercubic lattice in d dimension, we can write the dimension-dependent expression for the excluded volume of sticks,

$$V_{ex} = (2d - 1)(2k_1 - 1) + 1. \tag{9}$$

In this case, as the length of the sticks tends to infinity, we get the limiting threshold value in d dimensions as

$$\phi_c = 1 - \exp\left(-B_c \frac{1}{2(2d - 1)}\right). \tag{10}$$

Now, for the continuum problem where aligned hypercubes are placed randomly in d-dimensional space, we have the percolation threshold $\phi_c = 1 - \exp\left(-B_c \frac{1}{2^d}\right)$ [27]. Assuming B_c to be the same, we have the curious observation that the percolation threshold of sticks whose length tends to infinity and that of hypercubes (squares in 2D) whose sides tend to infinity have the same value in $d \approx 3.66$ dimensions. In other words, for dimensions three and less, the percolation threshold of the infinite hypercubes is larger than that of infinite sticks, whereas for dimensions greater than three, the percolation threshold of infinite sticks is larger than that of infinite hypercubes.

We can see that similar results, as discussed above, will also hold for other lattices. For example, on a triangular lattice, for objects of width k_2 and length k_1 (a "parallelogram") (see Fig. 4), $V_{ex} = (2k_1 + 1)(2k_2 + 1) - 3$. In this case, we can see that ϕ_c is independent of k_1 for $k_2 = 1$ (sticks). Considering the limit $k_1 \to \infty$, we get $\phi_c = 1 - \exp(-B_c \frac{1}{6})$, whereas, if we consider parallelograms of equal sidelengths, say $k_1 = k_2 = k$, we get $\phi_c = 1 - \exp(-B_c \frac{1}{4})$ in the limit of $k \to \infty$.
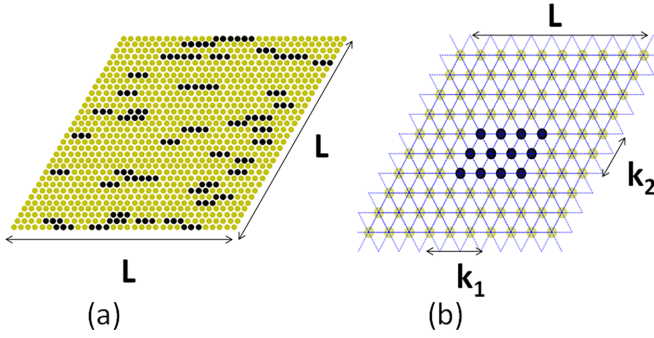
FIG. 4. (a) Overlapping trimers (sticks of length $k_1 = 3$ and width $k_2 = 1$) on a triangular lattice. (b) A parallelogram of $k_1 = 4$ and $k_2 = 3$ on a triangular lattice. The excluded volume will be $V_{ex} = (2k_1 + 1)(2k_2 + 1) - 3$.

The above results show that on N-dimensional lattices, when we are considering the percolation of aligned overlapping shapes that can be described by M independent length parameters, the following holds. (a) For a specific choice of values for $(M - 1)$ of these parameters, the percolation threshold can become independent of the remaining parameter. (b) Whenever we let a subset of the M parameters go to infinity while keeping the remaining parameters finite, we expect a finite percolation threshold, which depends upon the finite parameter values. (c) These limiting threshold values, in general, will differ from the corresponding continuum results.

We can perform the excluded volume theory calculations for other shapes in Fig. 1(c). For diamonds of size k [see Fig. 1(c)], the area of the diamond is $V = (\frac{k^2+1}{2})$, where k must be odd. If we choose the central site of the diamond as the index site, the shape of the excluded area will be a bigger diamond of size $(2k + 1)$. We can calculate the areas and excluded areas of isosceles triangles, and hexagons in a similar way. If we choose the central site of the base of the isosceles triangle as the index site, the shape of the excluded area will be a hexagon of dimensions $(2k + 1)$ and $(k + 1)/2$. For the hexagon, the shape of the excluded area will also be a hexagon of dimensions $(2k_1 + 1)$ and $(2k_2 + 1)$.

In Table I, we provide a summary of the expressions for the percolation thresholds obtained for a few different shapes using the discrete version of excluded volume theory. Wherever

possible, we have included numerical values for the limiting cases, where B_c values for different shapes are taken from existing studies of the continuum percolation problem of the corresponding shapes. Note that the diamond shape on an upright square lattice is equivalent to a square shape on a diagonal square lattice [56]. Hence we expect that the B_c values for the two are the same. In fact, Gouker and Family [57] have studied the percolation of diamond shapes on a square lattice. In Table II, we compare the theoretical predictions with the simulation values given in [57]. We can see an excellent agreement between the two at larger diamond sizes.

The following section presents simulation results for aligned and overlapping rectangles that closely agree with the predicted behavior. In particular, the agreement between the theory and simulation results seems exact for the limiting cases.

B. Simulation results

We simulate the model of aligned and overlapping rectangles on a two-dimensional square lattice and study its percolation properties. To construct the model, aligned rectangles of size $k_1 \times k_2$ are distributed uniformly and randomly on a square lattice of size $L \times L$. The percolation probability is determined by detecting the presence of a spanning cluster in the vertical direction using the standard Hoshen-Kopelman algorithm [58]. Later in Sec. III B 1, we verify that the results remain unchanged if we consider the horizontal direction for defining the spanning cluster. For each system size and density of occupied sites, we generate a number of samples and the percolation probability is evaluated as the fraction of samples that are percolating. The number of samples considered varies between 10^3 for $L \leqslant 256$ and 10^2 for higher values of L. Percolation probability is plotted against the density of occupied sites for different system sizes L and, by fitting each curve with the function $\frac{1+\text{erf}[\phi-\phi_c(L)/\Delta(L)]}{2}$, we obtain the effective percolation threshold $\phi_c(L)$ for system size L and width of the transition region $\Delta(L)$ [59]. We have the linear scaling relation,

$$\phi_c(L) = B * \Delta(L) + \phi_c(\infty), \qquad (11)$$

where $\phi_c(\infty)$ is the percolation threshold in the limit of infinite system size $L \rightarrow \infty$ and B is a constant [10]. A typical

TABLE I. Expressions for CCVF ϕ_c for various shapes and lattices from discrete excluded volume theory. For obtaining the numerical values in the last column, the B_c value for a shape is assumed to be that of the continuum percolation problem of the same shape.

Shape	Lattice	CCVF ϕ_c from discrete excluded volume theory	Limiting values of ϕ_c
Rectangles of size $k_1 \times k_2$	2D square	$1 - \exp(-B_c \frac{k_1 k_2}{(2k_1+1)(2k_2+1)-5})$	$1 - \exp(-B_c \frac{k_2}{4k_2+2})$ ($k_1 \rightarrow \infty$, finite k_2)
Squares ($k_1 = k_2 = k$)	2D square	$1 - \exp(-B_c \frac{k^2}{(2k+1)^2-5})$	0.6667 ($k \rightarrow \infty$), $B_c = 4.3953711(5)$ [27]
Diamonds of linear size k	2D square	$1 - \exp(-B_c \frac{k^2+1}{4k(k+1)})$	$1 - \exp(-B_c/4)$ ($k \rightarrow \infty$)
Triangles (isosceles of base k)	2D square	$1 - \exp(-B_c \frac{k^2+2k+1}{2(3k^2+6k-1)})$	$1 - \exp(-B_c/6)$ ($k \rightarrow \infty$)
Hexagon with dimensions k_1 and k_2	2D square	$1 - \exp(-B_c \frac{k_1+2k_2(k_1-k_2-1)}{(2k_1+1)+2(2k_2+1)(2k_1-2k_2-1)-1})$	$1 - \exp(-B_c \frac{k_2}{4k_2+2})$ ($k_1 \rightarrow \infty$, finite k_2)
Cubes ($k_1 = k_2 = k_3 = k$)	3D cubic	$1 - \exp(-B_c \frac{k^3}{(2k-1)^3+6(2k-1)^2-1})$	0.2773 ($k \rightarrow \infty$), $B_c = 2.5978(5)$ [27]
Sticks of length k_1	3D cubic	$1 - \exp(-B_c \frac{k_1}{5(2k_1-1)+1})$	0.22877 ($k_1 \rightarrow \infty$), $B_c = 2.5978(5)$ [27]
Parallelograms of size $k_1 \times k_2$	2D triangular	$1 - \exp(-B_c \frac{k_1 k_2}{(2k_1+1)(2k_2+1)-3})$	$1 - \exp(-B_c \frac{k_2}{4k_2+2})$ ($k_1 \rightarrow \infty$, finite k_2)

TABLE II. Comparison of discrete excluded volume theory results for diamond shapes on a square lattice with previous simulation results [57]. p_c is the critical number of objects per site and is related to $\phi_c = 1 - \exp(-\eta_c)$ via the relation $p_c = \frac{4\eta_c}{z}$ [31]. Interaction range R in [57] is related to k by $k = 2R + 1$. z is the coordination number [57].

k	ϕ_c using the expression in the third row of Table I	z	p_c	Simulation results for p_c from previous studies [57]
5	0.61416	12	0.3174	0.290 ± 0.005
9	0.63255	40	0.100117	0.105 ± 0.005
13	0.6417	84	0.04888	0.049 ± 0.005
17	0.6470	144	0.028927	0.028 ± 0.005
21	0.6505	220	0.01911	0.019 ± 0.005

example of the plot of percolation probability against the density of occupied sites for $k_1 = 3$, $k_2 = 1$ rectangles for different values of L and the corresponding plot of $\phi_c(L)$ against $\Delta(L)$ is shown in Fig. 5. Y intercept of the latter plot gives the percolation threshold in the $L \to \infty$ limit. The percolation threshold is determined for rectangles of widths $k_2 = 1$, 2, and 3 for increasing values of k_1 and is shown in Table III along with the values based on the lattice version of excluded volume theory discussed in Sec. III A. For the value of B_c, we take that obtained from continuum simulations of aligned squares or rectangles [$B_c = 4.3953711(5)$ [27]] to get numerical estimates of percolation thresholds.

Plots of the percolation threshold against k_1 for rectangles of width $k_2 = 1$, 2, and 3 are shown in Fig. 6, confirming the trends predicted by the theory. As predicted by the excluded volume theory, for $k_2 = 1$, the CCVF is monotonically decreasing, whereas for $k_2 = 3$, it is monotonically increasing with k_1. For $k_2 = 2$, critical density is nearly a constant. Percolation thresholds for the limiting case of $k_1 \to \infty$ are also shown in the figure.

1. Isotropy of percolation threshold

When considering $k_1 \times k_2$ rectangles on the square lattice, we fixed k_2 and varied k_1. For $k_1 > k_2$, this means that there is a preferred direction for the percolation to happen in finite systems; i.e., along the horizontal direction. In the last section, we defined the system as percolating when

there is a spanning cluster in a direction perpendicular to the direction of alignment. A natural question is whether the percolation point is different if we define a configuration as percolating when there is a spanning cluster in the direction of alignment. In continuum percolation models, previous studies suggest isotropy of the percolation threshold even for highly anisotropic systems like rectangles with large aspect ratios [51]. It is found that the effective percolation threshold for a finite system size in the direction of alignment will always be smaller compared to that in the orthogonal direction. However, this difference will decrease with increasing system size and finally vanish in the infinite system size limit. We verify that this isotropy of the percolation threshold holds for aligned rectangles on the square lattice as well. The critical density of occupied sites evaluated (see Fig. 7) shows that the percolation threshold is also isotropic in the case of lattices. Just as in the continuum case, this isotropy may be explained based on the uniqueness of the spanning cluster in percolation problems [51].

2. Critical exponents for aligned stick model

Critical exponents are evaluated using finite size scaling methods [9,10]. If $S_{\max}$ is the size of the largest cluster and S is the total size of the remaining clusters, we have the scaling relations,

$$S_{\max} \sim L^{d_f}, \tag{12}$$
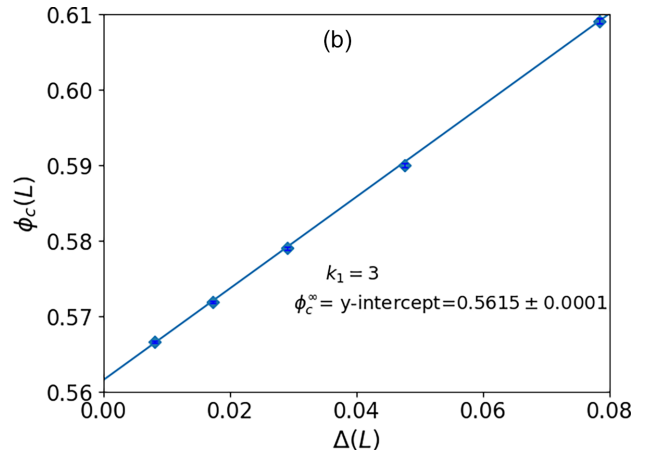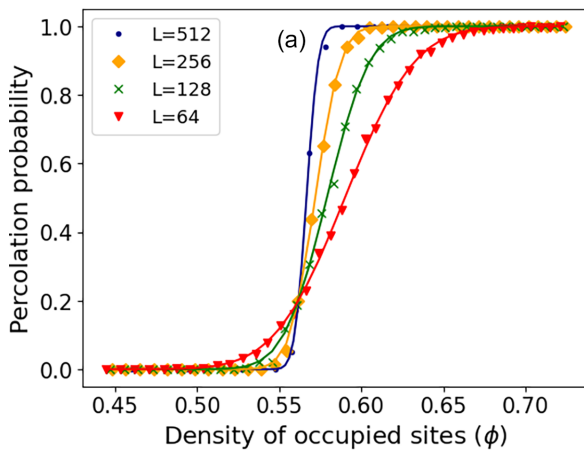
$$S \sim L^{\frac{\gamma}{\nu}}, \tag{13}$$

FIG. 5. (a) Variation of the percolation probability with the density of occupied sites ϕ for $k_1 = 3$, $k_2 = 1$ rectangles for different system sizes L. Solid lines are best-fit functions (see text). (b) Variation of the corresponding effective percolation threshold ϕ_c^L with the width of the transition region $\Delta(L)$ along with the best straight-line fit. Y intercept of the graph yields the threshold in the limit of infinite system size.

TABLE III. Percolation thresholds of aligned and overlapping rectangles of length k_1 and width $k_2 = 1$, 2, and 3 on a square lattice determined from simulations. The corresponding results from the discrete excluded volume theory for $k_2 = 2$ and 3 are also given for comparison. For $k_2 = 2$, the theory gives a constant value for $\phi_c^{k_1} = 0.5848$.

Length k_1	$\phi_c^{k_1}$, $k_2 = 1$	$\phi_c^{k_1}$, $k_2 = 1$ theory	$\phi_c^{k_1}$, $k_2 = 2$	$\phi_c^{k_1}$, $k_2 = 3$	$\phi_c^{k_1}$, $k_2 = 3$ theory
1	0.5927(4)	0.6667			
2	0.5715(18)	0.5848	0.5837(2)		
3	0.5615(1)	0.5614	0.5864(5)	0.5948(6)	0.5930
4	0.5523(9)	0.5503	0.5903(5)	0.5965(4)	0.5972
5	0.5497(19)	0.5438	0.5916(5)	0.597(2)	0.5997
7	0.5422(6)	0.5366	0.5909(26)	0.603(3)	0.6027
9	0.5402(46)	0.5326	0.5933(8)	0.6048(7)	0.6043
11	0.540(1)	0.5302	0.5922(27)	0.605(2)	0.6053
13	0.539(4)	0.5285	0.5950(16)	0.606(2)	0.6061
15	0.538(4)	0.5272	0.592(4)	0.608(2)	0.6066
17	0.536(4)	0.5263	0.593(7)	0.609(2)	0.6070
19	0.529(6)	0.5255	0.5927(41)	0.609(1)	0.6073
21	0.528(7)	0.5249	0.5928(14)	0.6102(1)	0.6076

where d_f is the fractal dimension, γ is the exponent corresponding to mean cluster size, and ν is the correlation length exponent. The plots of $S_{\max}$ against system size L and S against L for $k_1 = 3$, $k_2 = 1$ are shown in Figs. 8(a) and 8(b), respectively. The slopes of log-log plots give the fractal dimension $d_f = 1.90 \pm 0.04$ and the ratio $\frac{\gamma}{\nu} = 1.77 \pm 0.06$. The percolation probability $P(\phi, L)$ is expected to scale with the system size L as

$$P(\phi) = f((\phi - \phi_c)L^{\frac{1}{\nu}}), \tag{14}$$

where f is the scaling function. This implies that the curves of percolation probability for different L when plotted as a function of $(\phi - \phi_c)L^{\frac{1}{\nu}}$ with the correct value for ϕ_c and ν will collapse to a single curve. In Fig. 9(a), we verify that curves for various system sizes fall on top of each other for $\frac{1}{\nu} = 0.75$ and $\phi_c = 0.5615$.
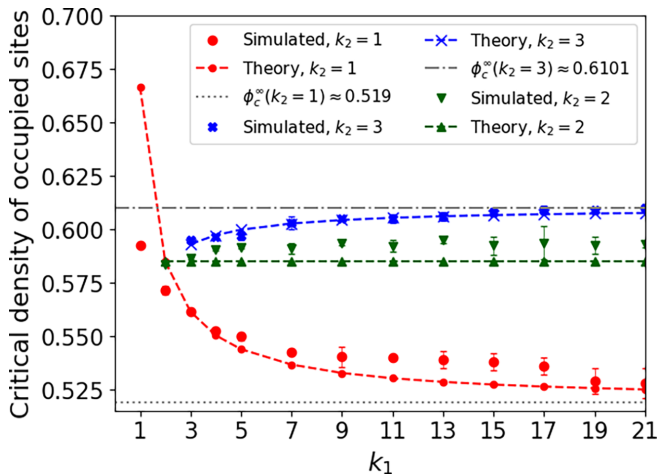
The other critical exponents are evaluated by making use of the relations

$$d_f = d - \frac{\beta}{\nu}, \tag{15}$$

$$\sigma = \frac{1}{\nu d_f}, \tag{16}$$

$$\tau = 1 + \frac{d}{d_f}. \tag{17}$$

We obtain $\nu \approx 1.33$, $\beta \approx 0.133$, $\sigma \approx 0.3948$, $\gamma \approx 2.36$, and $\tau \approx 2.05$. Finally, if $P_{\max}(\phi)$ is the probability of a site belonging to the largest cluster, it is expected to scale with the

FIG. 6. Percolation threshold ϕ_c vs k_1 for rectangles of width $k_2 = 1$, 2, and 3. Theoretical predictions for the thresholds based on the discrete excluded volume theory are also shown. The two horizontal lines (dotted for $k_2 = 1$ and dash-dotted for $k_2 = 3$) represent the thresholds in the limit $k_1 \to \infty$ obtained from Eq. (5).
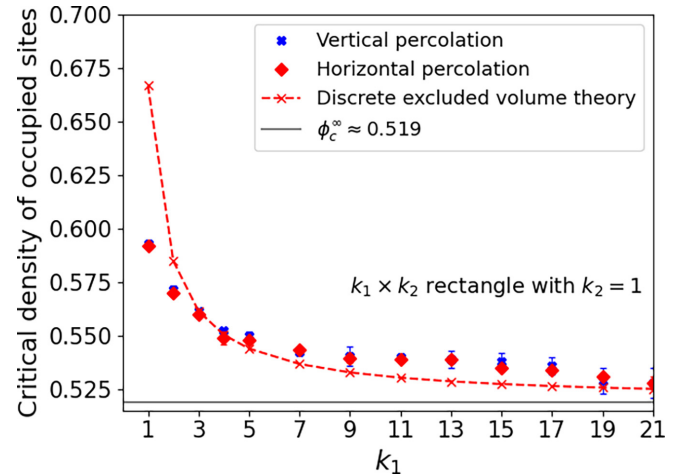

FIG. 7. Percolation threshold versus stick length k_1 for two different definitions of percolation. In one case, percolation is defined as the emergence of a spanning cluster in the vertical direction (perpendicular to the direction of alignment of sticks). In the other scenario, it is defined as the emergence of a spanning cluster in the horizontal direction (in the direction of alignment of sticks). Results from the excluded volume theory and the limiting value of the threshold for sticks of infinite length are also shown.
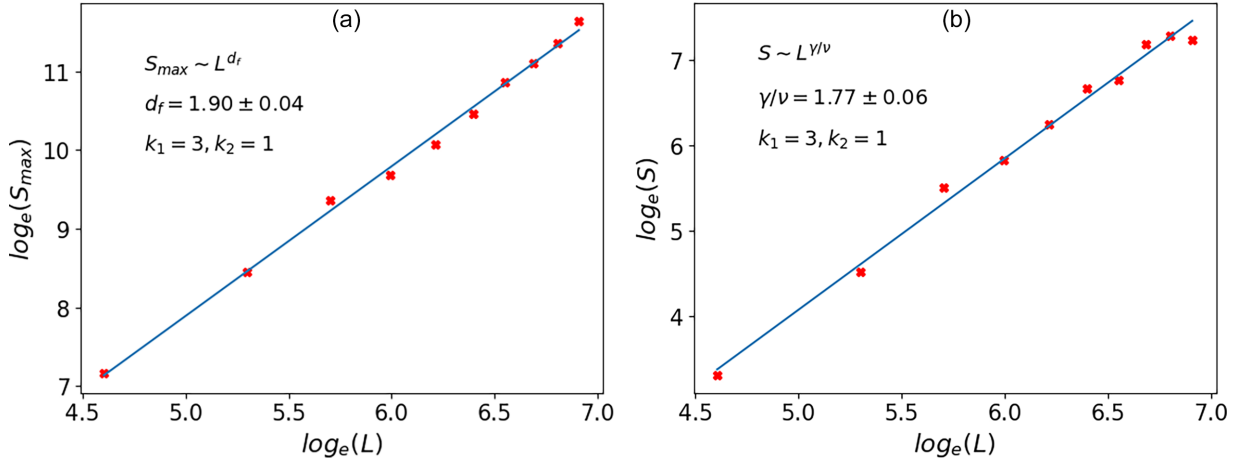
FIG. 8. (a) Variation of the size of the largest cluster $S_{\max}$ with system size L along with the best straight line fit for $k_1 = 3$, $k_2 = 1$. The slope of the log-log plot gives the fractal dimension d_f. (b) Variation of the size of the finite clusters S with system size L along with the best straight line fit. The slope of the log-log plot gives the ratio of critical exponents $\frac{\gamma}{\nu}$.

system size L as

$$P_{\max}(\phi) = L^{-\frac{\beta}{\nu}} F((\phi - \phi_c)L^{\frac{1}{\nu}}), \quad (18)$$

where F is the scaling function and β is the order parameter exponent. When $P_{\max}L^{\frac{\beta}{\nu}}$ is plotted against ϕ for different L, all curves will pass through a single point, which is at $\phi = \phi_c$ as verified in Fig. 9(b).

The obtained values of various critical exponents align with that of the standard two-dimensional percolation problem which are $\beta = 5/36$, $\gamma = 43/18$, $\nu = 4/3$, $\sigma = 36/91$, $\tau = 187/91$, and $d_f = 91/48$ [9]. Similar values are obtained for other values of k_1 and k_2 as well. Hence we can conclude that the percolation problem of aligned overlapping rectangles belongs to the standard percolation universality class. Note that the above results were obtained only for a limited range of k_1 and k_2 values. There remains the possibility that the value of the critical exponents could be different for higher values of k_1 and k_2, especially in the limiting cases of $k_1 \to \infty$ with finite k_2.

3. Comparison with rectangles of mixed orientation

We consider the percolation of overlapping sticks having both orientations (rectangles with $k_1 = 1$ or $k_2 = 1$ in our notation) here. The problem has been considered earlier in [30]. To study the percolation as we vary the relative fraction of sticks having horizontal and vertical orientations, we can define the parameter [19]

$$s = \frac{|(n_v - n_h)|}{|(n_v + n_h)|}, \quad (19)$$

where n_v and n_h represent the fraction of sticks that are vertically and horizontally oriented, respectively (see Fig. 10). Thus $s = 1$ corresponds to the fully aligned case and $s = 0$ corresponds to the isotropic case where the average fraction of sticks that are vertically and horizontally oriented is equal. The $s = 0$ case has been considered earlier in [30]. The values of the percolation threshold obtained for a few different values of the parameter s are given in Table IV along with the earlier results for the $s = 0$ case. We can see that the percolation threshold increases with an increase in the degree of
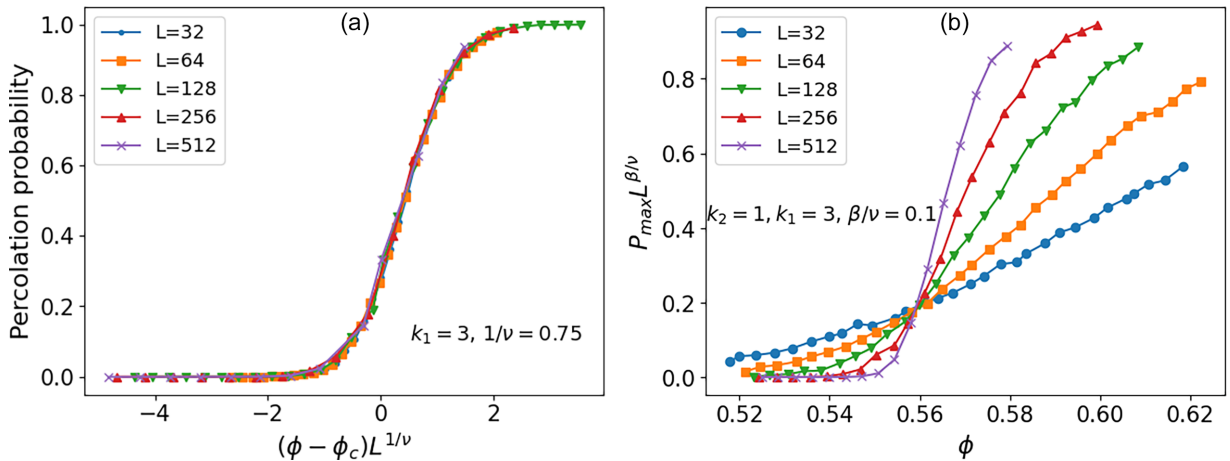

FIG. 9. (a) Plots of percolation probability against $(\phi - \phi_c)L^{\frac{1}{\nu}}$ for $k_1 = 3$, $k_2 = 1$ with $\frac{1}{\nu} = 0.75$ and $\phi_c = 0.5615$. (b) Plot of $P_{\max}L^{\beta/\nu}$ vs ϕ for $k_1 = 3$ and $k_2 = 1$ for $\frac{\beta}{\nu} = 0.1$, $\frac{1}{\nu} = 0.75$.

TABLE IV. Effect of alignment in dimer ($k = 2$ stick), trimer ($k = 3$ stick), and $k = 4$ stick percolation. The critical density of occupied sites ϕ_c for different values of s is shown. The values of ϕ_c for the special case of $s = 0$ from [30] are also given. Note that, in [30], the thresholds are given in terms of p_c, which is the critical number of objects per site. ϕ_c is related to p_c via the relation $\phi_c = 1 - (1 - p_c)^{2k}$. Theoretical values of ϕ_c calculated from the s-dependent excluded volume theory relation (see Appendix B) assuming $B_c \approx 4.3953711$ is given for comparison.

s	Length of the sticks	ϕ_c	ϕ_c for $s = 0$ from [30]	ϕ_c from theory (see Appendix B)
$s = 0$	2	0.5483(2)	0.54691	0.5503
$s = 0.66$	2	0.55885(14)		0.5651
$s = 1$	2	0.5715(18)		0.5848
$s = 0$	3	0.50004(64)	0.49898	0.5097
$s = 0.33$	3	0.5325(38)		0.5150
$s = 1$	3	0.5615(1)		0.5614
$s = 0$	4	0.4562(7)	0.45761	0.4785
$s = 0.33$	4	0.4665(2)		0.4855
$s = 0.66$	4	0.4944(17)		0.5081
$s = 1$	4	0.5523(9)		0.5503

alignment, which is also seen in earlier results for nonoverlapping sticks [19].

We can derive an s-dependent expression for the excluded area as well as ϕ_c for overlapping rectangles of mixed orientations on a square lattice. Details of the derivation and results are given in Appendix B. The results confirm that the interesting behavior observed for the thresholds for fully aligned rectangles is unique and we do not expect it for values of s different from 1 (fully aligned case). For $s < 1$, for large k_1, the percolation threshold is found to be a monotonically decreasing function of k_1. Theoretical values obtained from the s-dependent expression for ϕ_c in Appendix B are also given in Table IV for comparison. Even with the low values of length considered, the deviation from simulation results is typically a few percent, with the best accuracy seen for the fully aligned case ($s = 1$) where the deviation is typically less than 1%.

4. Discrete to continuum transition

Models of extended shapes on lattices interpolate between discrete and continuum percolation models. With symmetric shapes like squares, letting the size of the squares go to infinity—which is equivalent to letting the lattice spacing go

FIG. 10. (a) Horizontal and vertical dimers on a 50×50 square lattice with the density of occupied sites 0.5. $s \approx 0$. (b) Horizontal and vertical dimers on a 50×50 square lattice with $s \approx 0.66$. The gray color corresponds to the dimers.

to zero, for an infinite lattice—yields the continuum limit [28]. The convergence of discrete hypercubes and hyperspheres to corresponding continuum models and the universality of the convergence rate is discussed in [28,29]. However, with anisotropic shapes like rectangles considered here, letting the length of one side of the shape go to infinity while keeping the other side fixed—similar to letting the lattice spacing go to zero only along one direction—does not seem to correspond to any usual continuum percolation problem. Note that the continuum percolation threshold for aligned rectangles of all aspect ratios is the same as that of aligned squares [51]. However, as we saw, no corresponding result exists for lattices. Just to emphasize the difference in values, we find the limiting value of a 2D stick percolation model to be $\phi_c^\infty \approx 0.519$, whereas the continuum percolation threshold for aligned rectangles is $\phi_c \approx 0.667$ [51]. Similarly, in three dimensions, we find the limiting value of the 3D stick model to be $\phi_c \approx 0.229$, whereas the continuum percolation threshold value for overlapping cubes is $\phi_c \approx 0.277$ [13].

The appropriate "continuum" analog of the case where we let the length of the rectangles on the lattice go to infinity while keeping its width finite can be seen as a semicontinuum system in which rectangles are dropped into parallel lanes. The rectangles can be placed anywhere in each lane (horizontal direction), but they cannot straddle between the lanes. A schematic representation of the system for two different widths of the rectangles is shown in Fig. 11.
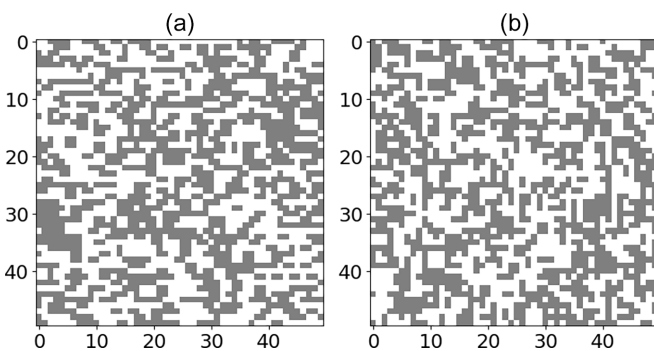
IV. CONCLUSIONS

Percolation of overlapping and extended shapes on lattices that interpolate between discrete and continuum models is a topic of recent interest. This work investigates the percolation of aligned, overlapping, and anisotropic shapes on lattices. First, we use a lattice version of excluded volume theory to show that shape anisotropy leads to some intriguing consequences regarding the percolation behavior. As a quintessential example of an anisotropic object, we investigate the case of aligned and overlapping rectangles on a square lattice in detail and show that, for rectangles of width unity (sticks), the percolation threshold is a monotonically
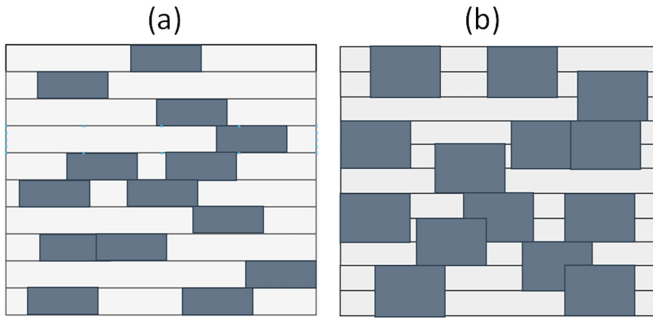
FIG. 11. Schematic representation of a percolation model of aligned, overlapping rectangles on a 2D semicontinuum geometry. The darker color corresponds to the rectangles. Rectangles whose widths are restricted to integer multiples of lane width are dropped into lanes with a specific number density. Two rectangles are considered connected if they overlap or share an edge. (a) Rectangles with width $k_2 = 1$. (b) Rectangles with width $k_2 = 2$.

decreasing function of the stick length. In contrast, for rectangles of width greater than two, the percolation threshold is a monotonically increasing function of the length. The percolation threshold is independent of its length for rectangles of width two. This independence of threshold on the length of a side holds for d-dimensional hypercubiods as well for specific integer values for the lengths of the remaining sides. The limiting case of the length of the rectangles going to infinity shows some remarkable behavior. It is found that the limiting value depends upon the rectangle's width. This is in stark contrast to the continuum percolation of aligned overlapping rectangles for which the percolation threshold is independent of the aspect ratio. The general notion that continuum percolation of aligned objects can be considered the limiting case of a corresponding discrete model [28] is only valid for symmetric shapes. Our research extends beyond rectangles, demonstrating that similar results hold for anisotropic objects on various lattices and dimensions and giving trends and numerical estimates of percolation thresholds for several such shapes and lattices.

We present simulation results for the percolation thresholds, which verify the predictions of the excluded volume theory. The percolation thresholds from simulations show that the lattice-excluded volume theory gives very good numerical estimates and its accuracy increases with the size of the extended shapes. We also determine the critical exponents for the model using simulations, which confirm that the model with finite rectangles belongs to the same universality class as the usual lattice percolation.

In addition, we verify the isotropy of the percolation threshold by obtaining the thresholds for percolation transition with the spanning cluster considered in the direction of alignment and the orthogonal direction. We also compare our results with models where rectangles of mixed orientation are allowed and models where nonoverlapping sticks with varying degrees of anisotropy are considered. Our simulation results show that alignment increases the percolation threshold even for overlapping shapes.

The findings of this study contribute to a deeper understanding of percolation behavior in lattice systems with

overlapping shapes and shed light on the intricate interplay between discrete and continuum models. Our results show that the lattice version of the excluded volume theory is remarkably accurate in describing the behavior of percolation of aligned and overlapping shapes on lattices qualitatively and quantitatively.

Our study opens up many avenues for further research. In this work, for obtaining the numerical results for the thresholds using the discrete excluded volume theory, we used the value of B_c—the average number of connections an object has at the critical point—from continuum percolation. This essentially assumes that the connectivity properties of the lattice system of overlapping shapes are the same as that of the corresponding continuum system at the critical point. In other words, we are assuming that the connectivity network formed at critical points by discrete systems like the one we considered here is similar to the continuum critical network of similar shapes. It is desirable to obtain the value of B_c based on considerations of the lattice system itself. Methods like the ones discussed in [50,60–63] may provide alternate ways of looking into this problem.

Other factors like polydispersity of anisotropic shapes will affect the critical behavior of the percolation problem discussed [18]. Especially the effect of unbounded size distributions on the critical behavior is a problem of interest [64,65]. Another potential area for further investigation is the relation to extended neighborhood percolation models [31]. The "continuum" limiting case of the lattice percolation models considered here can be seen as percolation models on semicontinuum geometries (Fig. 11) where basic percolating units can occupy only positions in lanes, which is another interesting problem worth investigating. This semicontinuum model of percolation may have relevance in describing random geometry of materials with a layered structure, such as layered rocks [66,67]. A detailed description and analysis of the model will be attempted in future work.

APPENDIX A: INDEPENDENCE OF PERCOLATION THRESHOLD ϕ_c ON SIDELENGTH k_1 FOR A PARTICULAR SET OF INTEGER VALUES OF SIDELENGTHS $k_2, k_3, k_4, \ldots, k_d$ FOR ALIGNED HYPERCUBOIDS ON A d-DIMENSIONAL HYPERCUBIC LATTICE

Consider hypercuboids with sidelengths $k_1, k_2, k_3, \ldots, k_d$ on a d-dimensional hypercubic lattice. Hypercuboids are randomly distributed and aligned along the direction of k_1. In Sec. III A, we showed that, in three dimensions, there is a unique set of integer values of k_2 and k_3, which will make the percolation threshold independent of k_1. Here, we generalize this result to d dimensions. We show that there is always a set of integer values of $k_2, k_3, \ldots, k_d$ such that the threshold is independent of k_1.

TABLE V. Integer solutions a_i and corresponding k_i values obtained for various dimensions d using Eq. (A6).

Dimension d	Values of $a_2, a_3, \ldots, a_d$	Set of integer solutions $k_2, k_3, \ldots, k_d$
2	3	2
3	3, 7	2, 4
4	3, 7, 43	2, 4, 22
5	3, 7, 43, 1807	2, 4, 22, 904
6	3, 7, 43, 1807, 3263443	2, 4, 22, 904, 1631722

Considering $(d-1)$ dimensions, assume that we have a set of integers $k_2, k_3, \ldots, k_{d-1}$ which makes ϕ_c independent of k_1. Let $a_i = (2k_i - 1)$ for $i = 1, 2, \ldots, (d-1)$. Then generalizing Eq. (7), the expression for the excluded volume of aligned hypercuboids in $(d-1)$ dimensions can be written as

$$V_{ex} = a_1 A_1 + 2[a_1 A_{d-1} + a_1 A_{d-2} + a_1 A_{d-3} + \cdots$$
$$+ \cdots a_1 A_4 + a_1 A_3 + a_1 A_2 + A_1] - 1, \quad (A1)$$

where

$$A_1 = \prod_{i=2}^{(d-1)} a_i$$

and

$$A_j = \prod_{i=2, i \neq j}^{(d-1)} a_i.$$

For ϕ_c to be independent of k_1, the ratio $\frac{V}{V_{ex}}$ should not contain any k_1 in it, which means that V_{ex} has to be a multiple of k_1. For this to happen, for a particular choice of integers $k_2, k_3, \ldots, k_{d-1}$, we will have an expression of the form $V_{ex} = B_1 a_1 + B_2$, where B_1 and B_2 are constants for a particular choice of $a_2, a_3, \ldots, a_{d-1}$. Now V_{ex} will be a multiple of k_1 if and only if $B_1 = B_2$. Identifying B_1 and B_2 from Eq. (A1) leads to the condition

$$2[A_{d-1} + A_{d-2} + A_{d-3} + \cdots + A_4 + A_3 + A_2] = A_1 - 1. \quad (A2)$$

Now assume that Eq. (A2) is satisfied in $(d-1)$ dimensions for a particular set of integer values $a_1, a_2, \ldots, a_{d-1}$. Using these values in the d-dimensional problem, we can write the expression for V_{ex} in d dimensions as

$$V_{ex} = a_1 A_1 a_d + 2[a_1 A_1 + a_1 A_{d-1} a_d + a_1 A_{d-2} a_d + \cdots$$
$$+ a_1 A_4 a_d + a_1 A_3 a_d + a_1 A_2 a_d + A_1 a_d] - 1, \quad (A3)$$

where a_d is still to be determined.

For ϕ_c to be independent of k_1, we now have the condition

$$2[A_1 + A_{d-1} a_d + A_{d-2} a_d + \cdots + A_4 a_d + A_3 a_d + A_2 a_d]$$
$$= A_1 a_d - 1. \quad (A4)$$

From this, we get

$$a_d = \frac{-(1 + 2A_1)}{[2(A_{d-1} + A_{d-2} + A_{d-3} + \cdots + A_3 + A_2) - A_1]}. \quad (A5)$$

Now using Eq. (A2) in this, we get

$$a_d = 1 + 2A_1. \quad (A6)$$

Since A_1 is a product of integers, a_d is always an odd positive integer. Since Eq. (A2) is satisfied in three dimensions, we can conclude that there is always a set of integer values for $k_2, k_3, \ldots, k_d$, which will make the percolation threshold of hypercuboids on a d-dimensional cubic lattice independent of k_1. Solutions obtained for a few dimensions are listed in Table V.

APPENDIX B: EXCLUDED VOLUME RESULTS FOR MULTIORIENTED RECTANGLES ON A SQUARE LATTICE

Consider a square lattice of size $L \times L$. N units of percolating objects are placed randomly. Each unit of percolating objects is a rectangle with sidelengths k_1 and k_2. Assume that $k_1 > k_2$. Assume that out of total N, n_v rectangles are placed vertically (i.e., side with size k_1 in the Y direction) and n_H are placed horizontally (i.e, side with size k_1 in the X direction). As in Sec. III B 3, we define a parameter $s = \frac{|n_v - n_h|}{n_v + n_h}$. Alternatively, if we define p_h as the probability of a rectangle being placed horizontally and p_v as the probability of a rectangle being placed vertically,

$$p_h = n_h/N, \quad (B1)$$

$$p_v = n_v/N = 1 - p_h. \quad (B2)$$

Then, parameter s can be written as

$$s = |p_v - p_h|. \quad (B3)$$

We can write the average excluded volume [68] of our system of multioriented rectangles as

$$V_{ex} = p_v p_v V_{ex}^{vv} + p_h p_h V_{ex}^{hh} + p_v p_h V_{ex}^{vh} + p_h p_v V_{ex}^{hv}, \quad (B4)$$

where V_{ex}^{vv} is the excluded volume of a vertical rectangle to another vertical rectangle (see Sec. III A for the definition of connectedness between shapes), V_{ex}^{hh} is the excluded volume of a horizontal rectangle to another horizontal rectangle, and $V_{ex}^{hv} = V_{ex}^{vh}$ is the excluded volume of a vertical rectangle to a horizontal one.

For multioriented rectangles of length k_1 and width k_2, we have

$$V_{ex}^{vv} = (2k_1 + 1)(2k_2 + 1) - 5,$$

$$V_{ex}^{hh} = (2k_1 + 1)(2k_2 + 1) - 5,$$

$$V_{ex}^{vh} = (k_1 + k_2 + 1)^2 - 4,$$

$$V_{ex}^{hv} = (k_1 + k_2 + 1)^2 - 4.$$

Using these in (B4), we get

$$V_{ex} = \left(\frac{1+s}{2}\right)^2 [(2k_1 + 1)(2k_2 + 1) - 5]$$

$$+ \left(\frac{1-s}{2}\right)^2 [(2k_1 + 1)(2k_2 + 1) - 5]$$

$$+ \frac{1-s^2}{4}[(k_1 + k_2 + 1)^2 - 4]$$

$$+ \frac{1-s^2}{4}[(k_1 + k_2 + 1)^2 - 4], \tag{B5}$$

which can be used in the expression for ϕ_c,

$$\phi_c = 1 - \exp\left(-B_c \frac{V}{V_{ex}(s)}\right). \tag{B6}$$

For $s = 1$, we recover the results described in Sec. III A. For all values of $s < 1$, from the above expression, we can easily verify that ϕ_c decreases monotonically for large k_1. The ratio $\frac{V}{V_{ex}}$ will depend inversely on k_1 for large k_1 and $k_1 \gg k_2$. Thus the peculiar behavior observed for the $s = 1$ (fully aligned) case is unique.

[1] M. Sahimi, *Applications of Percolation Theory* (Taylor and Francis, London, 1994).

[2] L. M. Sander, C. P. Warren, and I. M. Sokolov, Epidemics, disorder, and percolation, Physica A **325**, 1 (2003).

[3] J. Li, Z.-B. Zhang, and S.-L. Zhang, Percolation in random networks of heterogeneous nanotubes, Appl. Phys. Lett. **91**, 253127 (2007).

[4] C. Li and T.-W. Chou, Continuum percolation of nanocomposites with fillers of arbitrary shapes, Appl. Phys. Lett. **90**, 174108 (2007).

[5] B. Drossel and F. Schwabl, Forest-fire model with immune trees, Physica A **199**, 183 (1993).

[6] A. A. Klypin and S. F. Shandarin, Percolation technique for galaxy clustering, Astrophys. J. **413**, 48 (1993).

[7] M. Adam, M. Delsanti, J. P. Munch, and D. Durand, Sol-gel transition: A model for percolation, Physica A **163**, 85 (1990).

[8] D. Stauffer, Percolation models of financial market dynamics, Adv. Complex Syst. **04**, 19 (2001).

[9] K. Christensen. and N. R. Moloney, *Complexity and Criticality* (Imperial College Press, London, 2005).

[10] D. Stauffer and A. Aharony, *Introduction to Percolation Theory* (Taylor and Francis, London, 2018).

[11] S. Mertens and C. Moore, Continuum percolation thresholds in two dimensions, Phys. Rev. E **86**, 061109 (2012).

[12] W. Xia and M. F. Thorpe, Percolation properties of random Ellipses, Phys. Rev. A **38**, 2650 (1988).

[13] D. R. Baker, G. Paul, S. Sreenivasan, and H. E. Stanley, Continuum percolation threshold for interpenetrating squares and cubes, Phys. Rev. E **66**, 046136 (2002).

[14] E. T. Gawlinski and H. E. Stanley, Continuum percolation in two dimensions: Monte Carlo tests of scaling and universality for non-interacting discs, J. Phys. A: Math. Gen. **14**, L291 (1981).

[15] J. Becklehimer and R. B. Pandey, A computer simulation study of sticks percolation, Physica A **187**, 71 (1992).

[16] N. Vandewalle, S. Galam, and M. Kramer, A new universality for random sequential deposition of needles, Eur. Phys. J. B **14**, 407 (2000).

[17] P. Longone, P. M. Centres, and A. J. Ramirez-Pastor, Percolation of aligned rigid rods on two-dimensional square lattices, Phys. Rev. E **85**, 011108 (2012).

[18] Y. Y. Tarasevich and A. V. Eserkepov, Percolation of sticks: Effect of stick alignment and length dispersity, Phys. Rev. E **98**, 062142 (2018).

[19] Y. Y. Tarasevich, N. I. Lebovka, and V. V. Laptev, Percolation of linear k-mers on a square lattice: From isotropic through partially ordered to completely aligned states, Phys. Rev. E **86**, 061116 (2012).

[20] V. Cornette, A. J. Ramirez-Pastor, and F. Nieto, Dependence of percolation threshold on the size of percolating species, Physica A **327**, 71 (2003).

[21] V. Cornette, A. J. Ramirez-Pastor, and F. Nieto, Percolation of polyatomic species on a square lattice, Eur. Phys. J. B **36**, 391 (2003).

[22] W. Lebrecht, J. F. Valdés, E. E. Vogel, F. Nieto, and A. J. Ramirez-Pastor, Percolation of dimers on square lattices, Physica A **392**, 149 (2013).

[23] G. Kondrat and A. Pekalski, Percolation and jamming in random sequential adsorption of linear segments on a square lattice, Phys. Rev. E **63**, 051108 (2001).

[24] G. Kondrat, Impact of composition of extended objects on percolation on a lattice, Phys. Rev. E **78**, 011101 (2008).

[25] V. A. Cherkasova, Y. Y. Tarasevich, N. I. Lebovka, and N. V. Vygornitskii, Percolation of aligned dimers on a square lattice, Eur. Phys. J. B **74**, 205 (2010).

[26] P. Longone, P. M. Centres, and A. J. Ramirez-Pastor, Percolation of aligned rigid rods on two-dimensional triangular lattices, Phys. Rev. E **100**, 052104 (2019).

[27] Z. Koza, G. Kondrat, and K. Suszczyński, Percolation of overlapping squares or cubes on a lattice, J. Stat. Mech.: Theory Exp. (2014) P11005.

[28] Z. Koza and J. Pola, From discrete to continuous percolation in dimensions 3 to 7, J. Stat. Mech.: Theory Exp. (2016) 103206.

[29] P. Brzeski and G. Kondrat, Percolation of hyperspheres in dimensions 3 to 5: From discrete to continuous, J. Stat. Mech.: Theory Exp. (2022) 053202.

[30] K. R. Mecke and A. Seyfried, Strong dependence of percolation thresholds on polydispersity, Europhys. Lett. **58**, 28 (2002).

[31] Z. Xun, D. Hao, and R. M. Ziff, Site percolation on square and simple cubic lattices with extended neighborhoods and their continuum limit, Phys. Rev. E **103**, 022126 (2021).

[32] M. Majewski and K. Malarz, Square lattice site percolation thresholds for complex neighborhoods, Acta Phys. Pol. B **38**, 2191 (2007).

[33] A. Alvarez-Alvarez, I. Balberg, and J. P. Fernandez-Alvarez, Invariant percolation properties in some continuum systems, Phys. Rev. B **104**, 184205 (2021).

[34] I. Balberg, The physical fundamentals of the electrical conductivity in nanotube-based composites, J. Appl. Phys. **128**, 204304 (2020).

[35] F. Du, J. E. Fischer, and K. I. Winey, Effect of nanotube alignment on percolation conductivity in carbon nanotube/polymer composites, Phys. Rev. B **72**, 121404(R) (2005).

[36] X. Ni, C. Hui, N. Su, W. Jiang, and F. Liu, Monte Carlo simulations of electrical percolation in multicomponent thin films with nanofillers, Nanotechnology **29**, 075401 (2018).

[37] R. Ramasubramaniam, J. Chen, and H. Liu, Homogeneous carbon nanotube/polymer composites for electrical applications, Appl. Phys. Lett. **83**, 2928 (2003).

[38] L. Hu, D. S. Hecht, and G. Gruner, Percolation in transparent and conducting carbon nanotube networks, Nano Lett. **4**, 2513 (2004).

[39] L. Berhan and A. M. Sastry, Modeling percolation in high-aspect-ratio fiber systems. I. Soft-core versus hard-core models, Phys. Rev. E **75**, 041120 (2007).

[40] L. Berhan and A. M. Sastry, Modelling percolation in high aspect-ratio fiber systems. II. The effect of waviness on the percolation onset, Phys. Rev. E **75**, 041121 (2007).

[41] P. M. Adler, Transport processes in fractals. Stokes flow through Sierpinski carpets, Phys. Fluids **29**, 15 (1986).

[42] S. Saleh, J. E. Thovert, and P. M. Adler, Measurement of two-dimensional velocity fields in porous media by particle image displacement velocimetry, Exp. Fluids **12**, 210 (1992).

[43] Y. Li, F. Kazemifar, G. Blois, and K. T. Christensen, Micro-PIV measurements of multiphase flow of water and liquid CO_2 in 2-D heterogeneous porous micromodels, Water Resour. Res. **53**, 6178 (2017).

[44] L.-P. Tang, S. Yang, D. Liu, C. Wang, Y. Ge, L.-M. Tang, R.-L. Zhou, and H. Zhang, Two-dimensional porous coordination polymers and nano-composites for electrocatalysis and electrically conductive applications, J. Mater. Chem. A **8**, 14356 (2020).

[45] A. Koponen, M. Kataja, and J. Timonen, Tortuous flow in porous media, Phys. Rev. E **54**, 406 (1996).

[46] A. Koponen, M. Kataja, and J. Timonen, Permeability and effective porosity of porous media, Phys. Rev. E **56**, 3319 (1997).

[47] A. Koponen, M. Kataja, and J. Timonen, Simulations of single fluid flow in porous medium, Int. J. Mod. Phys. C **9**, 1505 (1998).

[48] M. Matyka, A. Khalili, and Z. Koza, Tortuosity-porosity relation in porous media flow, Phys. Rev. E **78**, 026306 (2008).

[49] Z. Koza, M. Matyka, and A. Khalili, Finite-size anisotropy in statistically uniform porous media, Phys. Rev. E **79**, 066306 (2009).

[50] K. R. Mecke, Additivity, convexity, and beyond: Applications of Minkowsky functionals in statistical physics, in *Statistical Physics and Spatial Statistics* (Springer, Berlin, 2000), pp. 111–184.

[51] M. A. Klatt, G. E. Schroder-Turk, and K. Mecke, Anisotropy in finite continuum percolation: Threshold estimation by Minkowsky functionals, J. Stat. Mech.: Theory Exp. (2017) 023302.

[52] D. Dhar, On the critical density for continuum percolation of spheres of variable radii, Physica A **242**, 341 (1997).

[53] I. Balberg, C. H. Anderson, S. Alexander, and N. Wagner, Excluded volume and its relation to the onset of percolation, Phys. Rev. B **30**, 3933 (1984).

[54] I. Balberg, Recent developments in continuum percolation, Philos. Mag. B **56**, 991 (1987).

[55] Z. Xun, D. Hao, and R. M. Ziff, Site and bond percolation on regular lattices with compact extended-range neighborhoods in two and three dimensions, Phys. Rev. E **105**, 024105 (2022).

[56] J. L. Bernard and R. Fred, *Numbers and Symmetry: An Introduction to Algebra* (CRC Press, New York, 1997).

[57] M. Gouker and F. Family, Evidence for classical critical behavior in long-range site percolation, Phys. Rev. B **28**, 1449 (1983).

[58] J. Hoshen and R. Kopelman, Percolation and cluster distribution. I. Cluster multiple labeling technique and critical concentration algorithm, Phys. Rev. B **14**, 3438 (1976).

[59] M. D. Rintoul and S. Torquato, Precise determination of the critical threshold and exponents in a three dimensional continuum percolation model, J. Phys. A: Math. Gen. **30**, L585 (1997).

[60] F. Coupette, R. de Bruijn, P. Bult, S. Finner, M. A. Miller, P. van der Schoot, and T. Schilling, Nearest-neighbor connectedness theory: A general approach to continuum percolation, Phys. Rev. E **103**, 042115 (2021).

[61] F. Coupette and T. Schilling, Exactly solvable percolation problems, Phys. Rev. E **105**, 044108 (2022).

[62] F. Coupette and T. Schilling, Universal approach to critical percolation, arXiv:2308.16757.

[63] K. R. Mecke, Integral geometry in statistical physics, Int. J. Mod. Phys. B **12**, 861 (1998).

[64] V. Sasidevan, Continuum percolation of overlapping disks with a distribution of radii having a power-law tail, Phys. Rev. E **88**, 022140 (2013).

[65] P. Hall, On continuum percolation, Ann. Probab. **13**, 1250 (1985).

[66] T. Bai, D. D. Pollard, and H. Gao, Explanation for fracture spacing in layered materials, Nature (London) **403**, 753 (2000).

[67] D. Xu, T. Han, and L.-Y. Fu, Seismic dispersion and attenuation in layered porous rocks with fractures of varying orientations, Geophys. Prospect. **69**, 220 (2021).

[68] K. Meeks, M. L. Pantoya, M. Green, and J. Berg, Extending the excluded volume for percolation threshold estimates in polydisperse systems: The binary disk system, Appl. Math. Model. **46**, 116 (2017).